

# Nonlinear Model Predictive Guidance for Tilt-Rotor UAV Performing Terrain-Following Flight for Mine Detection

*Sangmin Lee<sup>\*†</sup>, Hyeongwan Kang<sup>\*</sup> and Youdan Kim<sup>\*</sup>*

*<sup>\*</sup>Department of Aerospace Engineering, Seoul National University  
08826 Seoul, Republic of Korea*

*everlastingminii@gmail.com · rkdgudrhks7@gmail.com · ydkim@snu.ac.kr*

*<sup>†</sup>Corresponding author*

## Abstract

A guidance law based on the nonlinear model predictive control method is designed for a tilt-rotor unmanned aerial vehicle (UAV) to perform terrain-following flight for landmine detection. Continuous terrain elevation model is constructed by applying the least square method to the data extracted from a digital elevation model. The guidance law is designed to minimize the altitude tracking error of the UAV considering the constraints arising from the characteristics of the landmine detection mission and the physical limitations of the UAV. Numerical simulation is performed to demonstrate the effectiveness of the proposed method.

## 1. Introduction

Unmanned aerial vehicles (UAVs) have been used for various search missions because they can quickly explore large areas from the sky, which is relatively less constrained by ground obstacles than humans or ground vehicles. In addition, UAVs are safer when the target for the search mission has toxicity or the risk of explosion because UAVs can search the target at a certain distance. Particularly, finding landmines buried on the battlefield offers strategic value during wartime situations and is also necessary for safely removing the remaining landmines after the end of the war. To use a UAV for landmine detection, ensuring the accuracy of detection sensors mounted on the UAV is important. Magnetic field sensor<sup>6</sup> and chemical sensor are widely used as the detection sensor, each of which detects the landmine by measuring the strength of either the magnetic field or the concentration of chemicals. The measurement signal of the sensors varies depending on the distance between the UAV and the landmine. Also, the sensors should be always facing the ground in a direction perpendicular to the ground. Consequently, the UAV is required to perform a terrain-following flight while keeping its attitude constant to obtain accurate sensor signals. Generally, fixed-wing aircraft are not suitable for this purpose because fixed-wing aircraft should change their attitude to change the altitude. Multi-copters do not have the same problem, but they have to adjust their attitude frequently to fly at a constant horizontal speed under varying wind conditions. On the other hand, tilt-rotor UAVs are free from these restrictions.

Terrain-following flight is typically performed by generating a reference trajectory based on the terrain elevation data and then tracking the reference trajectory. Lu et al.<sup>2</sup> proposed a trajectory optimization for the terrain-following method, where the performance index was defined to minimize the flight time and the altitude above the ground. Malaek et al.<sup>3</sup> constructed a continuous terrain model from the terrain elevation data using Chebyshev polynomials and solved the minimum flight time problem. These studies commonly regarded the terrain as an obstacle that should be avoided or passed by the UAV, which means that the attitude of the UAV was not much of interest. In the landmine detection mission, however, the constraints arising from the necessity of maintaining the constant attitude should be considered when generating a reference trajectory or a guidance command.

In this study, a guidance law is designed for a tilt-rotor UAV to perform the landmine detection mission based on the model predictive control (MPC) method. The UAV has tiltable rotors as well as aerodynamic control surfaces, and therefore it can change the altitude without changing the attitude. The guidance law computes the guidance command by finding an optimal input sequence over a finite horizon, which is referred to as the prediction horizon, that makes the UAV follow the terrain with a constant clearance. The prediction model is constructed based on the equations of the longitudinal motion. In addition, approximated constraints reflecting the physical limitation of the vehicle are derived and included in the optimization problem.

The remaining sections are organized as follows. Section 2 briefly summarizes the mathematical model of the UAV and the terrain. Section 3 explains the prediction model, constraints, and cost function that are needed for the

## NONLINEAR MODEL PREDICTIVE GUIDANCE FOR TILT-ROTOR UAV

guidance algorithm. Section 4 analyzes the performance of the designed guidance law by performing the numerical simulation. Finally, Sec. 5 concludes the study.

## 2. Model

### 2.1 UAV Model

The tilt-rotor vehicle considered in this study is shown in Fig. 1.

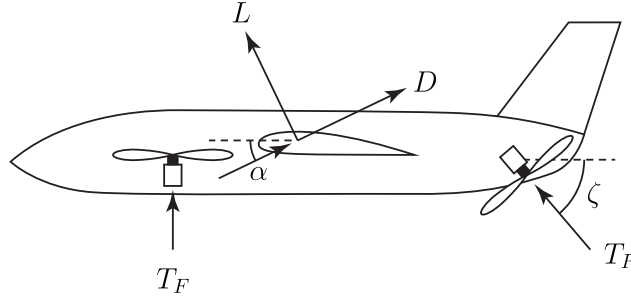


Figure 1: Tilt-rotor UAV

The vehicle has an elevator and a rudder as aerodynamic control surfaces, and two front rotors and two rear rotors for generating the thrust. The front rotors can only generate vertical thrust because they are rigidly attached to the fuselage. In contrast, the rear rotors can generate either vertical or horizontal thrust depending on the flight mode by changing the tilt angle  $\zeta$ . Specifically, the rear rotors are tilted to generate vertical thrust during the VTOL mode ( $\zeta = \frac{\pi}{2}$ ) and horizontal thrust during the fixed-wing mode ( $\zeta = 0$ ). Unlike a fixed-wing aircraft that adjusts the normal acceleration by changing its pitch angle, the vehicle can adjust the normal acceleration by changing the thrust of the front rotors with maintaining its pitch angle constant.

The longitudinal dynamics of the tilt-rotor vehicle in the fixed-wing mode can be expressed as follows,

$$m\dot{V}_T = T_R \cos \alpha - T_F \sin \alpha - D - mg \sin \gamma \quad (1)$$

$$m\dot{\gamma}V_T = T_R \sin \alpha + T_F \cos \alpha + L - mg \cos \gamma \quad (2)$$

$$\dot{q} = \frac{1}{J_y} M_y \quad (3)$$

$$\dot{\theta} = q \quad (4)$$

$$\dot{p}_x = V_T \cos \gamma \quad (5)$$

$$\dot{h} = V_T \sin \gamma \quad (6)$$

where  $V_T$  is the true airspeed,  $\gamma$  is the flight path angle,  $q$  is the pitch rate,  $\theta$  is the pitch angle,  $p_x$  is the downrange,  $h$  is the altitude,  $\alpha = \theta - \gamma$  is the angle of attack,  $T_R$  is horizontal thrust generated by the rear rotors,  $T_F$  is vertical thrust generated by the front rotors,  $D$  is the drag,  $L$  is the lift,  $M_y$  is the pitch moment,  $m$  is the mass,  $J_y$  is the y-axis moment of inertia, and  $g$  is the gravitational acceleration. Let  $C_D$  denote the drag coefficient and  $C_L$  denote the lift coefficient. The drag and lift can be expressed as

$$D = \frac{1}{2} \rho V_T^2 S C_D(\alpha, q, \delta_e) \quad (7)$$

$$L = \frac{1}{2} \rho V_T^2 S C_L(\alpha, q, \delta_e) \quad (8)$$

where  $\rho$  is the air density,  $S$  is the reference area, and  $\delta_e$  is the elevator deflection angle. The aerodynamic coefficients  $C_L$  and  $C_D$  are modeled as functions of  $\alpha$ ,  $q$ , and elevator deflection angle  $\delta_e$ .

### 2.2 Terrain Model

The terrain model is constructed from the actual terrain data provided on National Spatial Data Infrastructure Portal.<sup>4</sup> The data is provided as a digital elevation model (DEM) where grid points are spaced at regular intervals along the

North and East direction, and the terrain elevation is associated with the location of each grid point. Data processing is required before the data is exploited for computing the guidance command because the data contains the information only at discrete points. First, a horizontal path for the UAV is set on the terrain, and the terrain elevation is estimated at regular intervals along the path. Bilinear interpolation is used when estimating the terrain elevation at a point that does not belong to the grid points. Let  $p_{x,i}$  denote the downrange of the  $i$ -th ( $i = 1, 2, \dots, M$ ) point from the starting point measured along the path, and  $h_{t,i}$  denote the estimated terrain elevation at the point. The normalized downrange  $\hat{p}_{x,i}$  is defined as

$$\hat{p}_{x,i} = \frac{p_{x,i}}{L}, \quad (i = 1, 2, \dots, M) \quad (9)$$

where  $L$  denotes the length of the path. Then, a continuous elevation model can be constructed by applying the least square method to the estimated terrain elevation data  $(\hat{p}_{x,i}, h_{t,i})$  ( $i = 1, 2, \dots, M$ ), which is defined as a linear combination of cosine functions as

$$h_t = \sum_{k=0}^n c_k \cos(k\pi\hat{p}_x) \quad (10)$$

Each coefficient  $c_k$ , ( $k = 0, 1, \dots, n$ ), is determined by minimizing the sum of squared errors between the elevation calculated using the elevation model and the estimated elevation provided by the data. Let  $\mathbf{X}$  denote the matrix defined as

$$\mathbf{X} = \begin{bmatrix} 1 & \cos(\pi\hat{p}_{x,1}) & \cos(2\pi\hat{p}_{x,1}) & \cdots & \cos(n\pi\hat{p}_{x,1}) \\ \vdots & \vdots & \vdots & \ddots & \vdots \\ 1 & \cos(\pi\hat{p}_{x,M}) & \cos(2\pi\hat{p}_{x,M}) & \cdots & \cos(n\pi\hat{p}_{x,M}) \end{bmatrix} \quad (11)$$

Also, let  $\mathbf{c}$  denote the vector defined as  $\mathbf{c} = [c_0 \cdots c_n]^T$ , and  $\mathbf{y}$  denote the vector defined as  $\mathbf{y} = [h_{t,1} \cdots h_{t,M}]^T$ . The sum of the squared errors is expressed as

$$\text{Err} = \|\mathbf{y} - \mathbf{X}\mathbf{c}\|_2^2 \quad (12)$$

By minimizing (12), the coefficient vector  $c$  can be determined as

$$\mathbf{c} = (\mathbf{X}^T \mathbf{X})^{-1} \mathbf{X}^T \mathbf{y} \quad (13)$$

Figure 2 shows the elevation data and the elevation model constructed using the data with  $L = 2,700\text{m}$ ,  $M = 31$ , and  $n = 31$ .

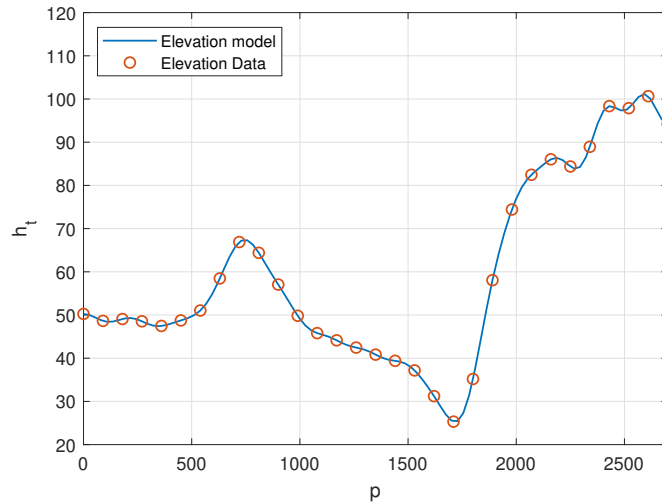


Figure 2: Elevation model constructed using the data

### 3. Guidance Law

#### 3.1 Prediction Model

Let us define pseudo-control inputs  $u_1$  and  $u_2$  from Eqs. (1) and (2) as

$$u_1 = T_R \cos \alpha - T_F \sin \alpha - D - mg \sin \gamma \quad (14)$$

$$u_2 = T_R \sin \alpha + T_F \cos \alpha + L - mg \cos \gamma \quad (15)$$

Then, equations related to the translational motion can be expressed as

$$\dot{p}_x = V_T \cos \gamma \quad (16)$$

$$\dot{h} = V_T \sin \gamma \quad (17)$$

$$m\dot{V}_T = u_1 \quad (18)$$

$$m\dot{\gamma}V_T = u_2 \quad (19)$$

Some limits should be imposed on the values of  $u_1$  and  $u_2$  according to Eqs. (14) and (15), respectively, and approximations are done to impose the proper limits in this study. If  $\alpha$  has a small value, the effect of  $T_R$  on  $u_1$  is much more than that of  $T_F$ . Therefore, the influence of  $T_F$  on  $u_1$  is negligible. Similarly, the influence of  $T_R$  on  $u_2$  is negligible when  $\alpha$  has a small value. Assuming that both  $\alpha$  and  $\gamma$  have small values,  $u_1$  and  $u_2$  can be approximated as

$$u_1 \approx T_R - D \quad (20)$$

$$u_2 \approx T_F + L - mg \quad (21)$$

For further simplification, the trim values for constant-speed level flight are derived based on Eqs. (1)-(6). Let  $\bar{V}_T$  denote the nominal speed of the vehicle, and let  $\bar{\alpha}$ ,  $\bar{q}$ , and  $\bar{\delta}_e$  denote the trim values of the angle of attack, pitch rate, and elevator deflection angle, respectively. The trim values can be computed by finding the solution that makes  $\dot{V}_T = 0$ ,  $\dot{\gamma} = 0$ ,  $\dot{q} = 0$ , and  $\dot{\theta} = 0$  under the conditions  $V_T = \bar{V}_T$  and  $\gamma = 0$ . Let us define the nominal drag  $\bar{D}$  and nominal lift  $\bar{L}$  on the trim condition as

$$\bar{D} = \frac{1}{2}\rho\bar{V}_T^2 S C_D(\bar{\alpha}, \bar{q}, \bar{\delta}_e) \quad (22)$$

$$\bar{L} = \frac{1}{2}\rho\bar{V}_T^2 S C_L(\bar{\alpha}, \bar{q}, \bar{\delta}_e) \quad (23)$$

Assuming that variations of  $D$  and  $L$  are relatively small compared to the variations of  $T_R$  or  $T_F$ ,  $u_1$  and  $u_2$  can be approximated as

$$u_1 \approx T_R - \bar{D} \quad (24)$$

$$u_2 \approx T_F + \bar{L} - mg \quad (25)$$

Note that  $T_R$  and  $T_F$  have limited values due to the physical limitations of rotors. Let us denote the range of  $T_R$  as  $[T_{R,\min}, T_{R,\max}]$ , and the range of  $T_F$  as  $[T_{F,\min}, T_{F,\max}]$ . Then, the limits imposed on  $u_1$  and  $u_2$  can be set as

$$T_{R,\min} - \bar{D} \leq u_1 \leq T_{R,\max} - \bar{D} \quad (26)$$

$$T_{F,\min} + \bar{L} - mg \leq u_2 \leq T_{F,\max} + \bar{L} - mg \quad (27)$$

In Eq. (19), the magnitude of  $\dot{\gamma}$  increases as  $V_T$  decreases for the same value of  $u_2$ , which implies that the vehicle can change its altitude more quickly by flying at a lower speed. However, flying at a lower speed also increases the risk of a stall and the total mission time required for searching the terrain. Therefore, a lower bound is set on  $V_T$  to prevent the vehicle from flying at an excessively low speed as follows,

$$V_T \geq V_{T,\min} \quad (28)$$

Dynamic equations in Eqs. (16)-(19) and constraints Eqs. (26)-(28) form the prediction model that is used for computing the guidance command, in which  $\mathbf{x} = [p_x \ h \ V_T \ \gamma]^T$  is considered as the state vector and  $\mathbf{u} = [u_1 \ u_2]^T$  is considered as the input vector.

### 3.2 Model Predictive Guidance

The objective of the guidance law is to ensure that the UAV follows the terrain maintaining a constant clearance from the ground and maintaining its speed close to the nominal speed  $\bar{V}_T$ . Let  $\mathcal{X}$  denote the set of feasible states  $\mathbf{x}$  satisfying the constraint Eq. (28) and  $\mathcal{U}$  denote the set of feasible inputs  $\mathbf{u}$  satisfying the constraints Eqs. (26) and (27). For  $\mathbf{x} \in \mathcal{X}$ ,  $\mathbf{u} \in \mathcal{U}$ , let us define the dynamic model  $f(\mathbf{x}, \mathbf{u})$  as

$$f(\mathbf{x}, \mathbf{u}) = \begin{bmatrix} V_T \cos \gamma \\ V_T \sin \gamma \\ \frac{1}{m} u_1 \\ \frac{1}{m V_T} u_2 \end{bmatrix} \quad (29)$$

The dynamic model is discretized with time interval  $\Delta t$  using the Runge-Kutta 4th order method. Let  $\mathbf{x}_k$  and  $\mathbf{u}_k$  denote the state and input at some time instant  $t_k$ , respectively. Then, the state  $\mathbf{x}_{k+1}$  at the next time instant  $t_{k+1} = t_k + \Delta t$  can be obtained by integrating the differential equation

$$\dot{\mathbf{x}} = f(\mathbf{x}, \mathbf{u}) \quad (30)$$

for time interval  $\Delta t$  with setting the initial condition as  $\mathbf{x}_k$  and applying the input  $\mathbf{u}_k$ . The step size for the Runge-Kutta 4th order method is set as the same value with the discretization time interval  $\Delta t$ . The mapping from  $\mathbf{x}_k$  and  $\mathbf{u}_k$  to  $\mathbf{x}_{k+1}$  can be represented as

$$\mathbf{x}_{k+1} = f_d(\mathbf{x}_k, \mathbf{u}_k) \quad (31)$$

Let  $h_c$  denote the desired clearance of the vehicle from the ground. Then, the reference altitude  $h_r$  for the vehicle can be defined as

$$h_r = h_t + h_c \quad (32)$$

A cost function  $J(\mathbf{x}, \mathbf{u})$  is defined by giving a penalty on the difference between the actual altitude and the reference altitude, a penalty on the difference between the actual speed and the nominal speed, and a penalty on  $u_1$  and  $u_2$  as follows,

$$J(\mathbf{x}, \mathbf{u}) = w_{V_T} (V_T - \bar{V}_T)^2 + w_h (h - h_r)^2 + w_{u_1} u_1^2 + w_{u_2} u_2^2 \quad (33)$$

where  $w_{V_T}$ ,  $w_h$ ,  $w_{u_1}$ , and  $w_{u_2}$  are the weights. Finally, the guidance law computes an optimal sequence  $\mathbf{U}^* = \{\mathbf{u}_0^*, \mathbf{u}_1^*, \dots, \mathbf{u}_{N-1}^*\}$  that minimizes the cost function  $J(\mathbf{x}, \mathbf{u})$  over a finite horizon of  $N$  time steps as<sup>1</sup>

$$\mathbf{U}^* = \arg \min_{\mathbf{U}} \sum_{k=0}^{N-1} J(\mathbf{x}_k, \mathbf{u}_k) \quad (34)$$

subject to  $\mathbf{x}_{k+1} = f_d(\mathbf{x}_k, \mathbf{u}_k)$ ,  $\mathbf{x}_k \in \mathcal{X}$ ,  $\mathbf{u}_k \in \mathcal{U}$

## 4. Numerical Simulation

Numerical simulation is performed to demonstrate the effectiveness of the proposed guidance law. The dynamic model described in Eqs. (16)-(19) is used as a simulation model. The parameters for the simulation model are summarized in Table. 1.

Table 1: UAV model parameters

Parameters	Symbols	Values
Mass	$m$	18.7 kg
Nominal speed	$\bar{V}_T$	25 m/s
Nominal drag and lift	$\bar{D}, \bar{L}$	22.9 N, 172.6 N
Minimum thrusts	$T_{R,\min}, T_{F,\min}$	0 N, 0 N
Maximum thrusts	$T_{R,\max}, T_{F,\max}$	75 N, 45 N
Minimum speed	$V_{T,\min}$	22 m/s

The continuous elevation model shown in Fig. 2 is used as the terrain model. The clearance  $h_c$  is set as 30 m. Let us define  $h_0$  as the sum of the terrain elevation at the starting point and  $h_c$ . The initial condition of the UAV is set as  $\mathbf{x}_0 = [25 \ 0 \ 0 \ h_0]^T$ . The guidance law is implemented using MPCTools,<sup>5</sup> and the parameters for the guidance law are summarized in Table. 2.

Table 2: Guidance algorithm parameters

Parameters	Symbols	Values
Discretization interval	$\Delta t$	0.1 s
Clearance	$h_c$	30 m
Weights	$w_{V_T}, w_h, w_{u_1}, w_{u_2}$	0.01, 1, 0.0016, 0.0016
Prediction horizon length	$N$	20

Figures 3 and 4 show the results of the simulation. Figure 3 shows the altitude, true airspeed  $V_T$ , and altitude tracking error  $e_h = h_r - h$  with respect to the downrange, which shows that the UAV follows the terrain with minor tracking errors for most of the flight. Also, it shows that the UAV flies at a lower speed than  $\bar{V}_T$  when the slope of the terrain is steep. Figure 4 shows the control inputs  $u_1$  and  $u_2$  with respect to the downrange, which shows that appropriate values for the inputs are computed using the guidance law.

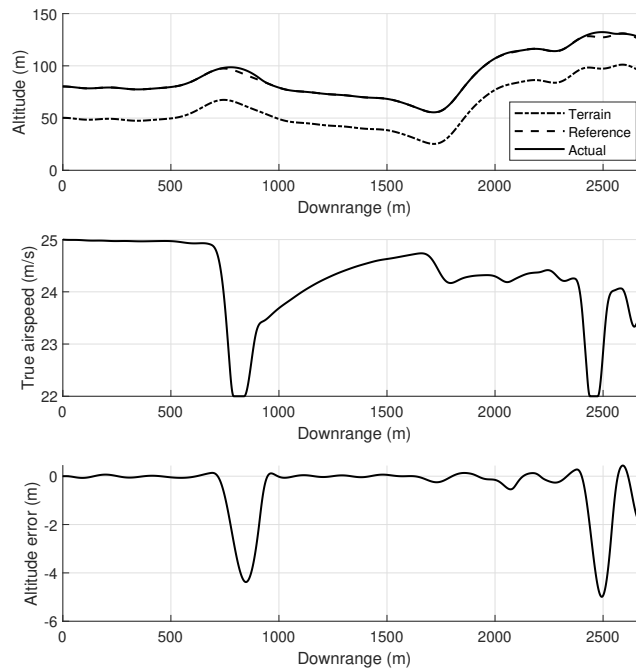


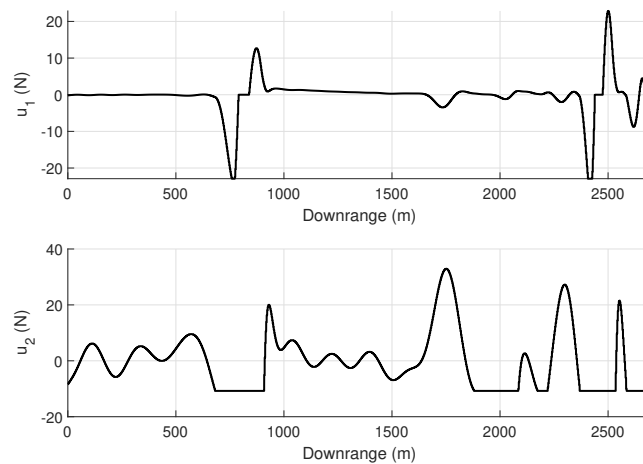
Figure 3: Altitude, true airspeed, and altitude error

## 5. Conclusion

A guidance law for a UAV performing a landmine detection was designed by applying the model predictive control method. Numerical simulation was performed to demonstrate the effectiveness of the proposed method. Numerical simulation results show that the proposed method makes the UAV fly above the ground at a certain clearance while keeping its speed close to the nominal speed. In future work, the performance of the proposed method will be analyzed on the longitudinal model with an attitude controller. Also, a more accurate approximation for the input constraints will be considered.

## 6. Acknowledgments

This research has been supported by the Defense Challengeable Future Technology Program of the Agency for Defense Development, Republic of Korea.

Figure 4: Inputs  $u_1$  and  $u_2$ 

## References

- [1] L. Bauersfeld, L. Spannagl, G. J. J. Ducard, and C. H. Onder. Mpc flight control for a tilt-rotor vtol aircraft. *IEEE Transactions on Aerospace and Electronic Systems*, 57(4):2395–2409, 2021.
- [2] P. Lu and B. L. Pierson. Optimal aircraft terrain-following analysis and trajectory generation. *Journal of guidance, Control, and Dynamics*, 18(3):555–560, 1995.
- [3] S. M. Malaek and A. R. Kosari. Novel minimum time trajectory planning in terrain following flights. *IEEE Transactions on Aerospace and Electronic Systems*, 43(1):2–12, 2007.
- [4] Ministry of Land, Infrastructure and Transport. National spatial data infrastructure portal. <http://www.nsdi.go.kr>, 2021.
- [5] M. Risbeck and J. Rawlings. Mpc tools: Nonlinear model predictive control tools for casadi. <https://bitbucket.org/rawlings-group/octave-mpc tools>, 2016.
- [6] L.-S. Yoo, J.-H. Lee, Y.-K. Lee, S.-K. Jung, and Y. Choi. Application of a drone magnetometer system to military mine detection in the demilitarized zone. *Sensors*, 21(9):3175, 2021.